Chemistry
A European
Journal

Chemistry Europe
European Chemical Societies Publishing

Accepted Article

Title: Hierarchical Synthesis, Structure, and Photophysical Properties of Gallium- and Ruthenium-Porphyrins with Axially Bonded Azo Ligands

Authors: Yueze Gao, Vroni Walter, Michael J. Ferguson, and Rik R. Tykwinski

To be cited as: *Chem. Eur. J.* 10.1002/chem.202002030

Link to VoR: https://doi.org/10.1002/chem.202002030

WILEY-VCH

10.1002/chem.202002030

Hierarchical Synthesis, Structure, and Photophysical Properties of Gallium- and Ruthenium-Porphyrins with Axially Bonded Azo Ligands

*Yueze Gao,[1] Vroni Walter,[2] Michael J. Ferguson,[1] and Rik R. Tykwinski[1,]**

[1]Department of Chemistry, University of Alberta, Edmonton, Alberta T6G 2G2 (Canada)
rik.tykwinski@uaberta.ca, orcid.org/0000-0002-7645-4784
[2]Department of Chemistry and Pharmacy & Interdisciplinary Center for Molecular Materials (ICMM), University of Erlangen-Nürnberg, Nikolaus-Fiebiger Str. 10, 91058 Erlangen (Germany)

Abstract: The hierarchical synthesis of three porphyrin and four bisporphyrin derivatives is presented. This strategy relies on the incorporation linkers based on azo moieties appended with pyridyl and/or acetylenic groups that facilitate axial coordination to Ga- and Ru-metalloporphyrins. These porphyrinic systems allow for a quantitative analysis of the effects of diamagnetic anisotropy (DA) using ^{1}H NMR spectroscopic and X-ray crystallographic analyses. A simple power-law relationship between the proton chemical shift and distance from the porphyrin core is experimentally outlined, which confirms previous theoretical predictions and shows that the limit of DA is about 2 nm. Photophysical properties of the azo-linked porphyrins are analyzed by UV-vis spectroscopy, showing that significant *cis-trans* isomerization is not observed for azo ligands bound only to Ga-porphyrins. Incorporation of Ru-porphyrins to an azo ligand facilitates photoswitching behavior, but the process faces competition from decarbonylation of the Ru-porphyrin, and appreciable switching is only documented for **GaL1Ru**.

Keywords: azo switches; alkynes; diamagnetic anisotropy; σ-acetylide; porphyrins

Introduction

Azobenzene derivatives have been developed as photoresponsive triggers in molecular machines,[1] biological systems,[2] and many other areas in which bistability is important.[3] In particular, the switchable nature of the azo group facilitates control of molecular configuration, and this allows a desired function to be fine-tuned.[4] Finally, the attachment of multicomponent, switchable systems to a surface is highly desirable to form functional nanosystems.[3a] As an elegant example, a "platform approach" has been developed by Herges and coworkers that allows for the organization of free-standing molecules on a Au surface, based on the design and synthesis of triazatriangulenium (TATA) moieties as the platform.[5]

As an alternative to triazatriangulenes as platforms,[6] porphyrins are flat, π-rich molecules, and they are well-known for constructing self-assembly on surfaces such as highly ordered pyrolytic graphite (HOPG) and metals.[7] Furthermore, metalloporphyrins can be readily modified through coordination of ligands to metal ions in the axial position.[8] Thus, the platform approach toward functional molecular nanostructures could be potentially advanced through the development of versatile protocols using porphyrins as platforms.

An intriguing system was recently reported by Hopkins and coworkers, which Ga-porphyrins were successfully assembled on the surface of HOPG.[9] This study utilized a simple metal acetylide ligand, which was placed in an orthogonal orientation to the surface through bonding to the platform. Intrigued by the concept of hierarchical assembly building from Ga-porphyrins, we have devised a protocol that allows a range of acetylides to be appended as ligands via axial bonding to a Ga-porphyrin.[10] The conjugation length and electronic composition of the ligands could be controlled through the selection of the alkyne chosen to form the acetylide, which allows strategic placement of further functionality above the surface.

Building on the concept of Ga-porphyrins as a platform, the attachment of photoresponsive groups as axial ligands was envisioned toward systems suitable for free standing surface functionalization. There have been examples reported of photoswitches attached to porphyrins, particularly the work of Herges and coworkers.[11] Furthermore, the tethering of two porphyrins

with an azo-bridge via either a *meso-meso*- or β-β-linkage has been explored,[12] as well as the supramolecular axial coordination of metalloporphyrins.[13] The direct attachment of an azo-switch via an axial covalent bond is rare and, to the best of our knowledge, limited to phosphorus porphyrins reported by Maiya et al.[14] and a Rh-porphyrin from Yao et al.[15]

Herein, we report an effective strategy to use axial bonding between the metal atom of a Ga-porphyrin and acetylide ligands bearing an azo moiety, toward creating a platform for switchable systems. The method is modular, allowing the hierarchical elaboration to form an unsymmetrical bisporphyrin via a coordination bond between an azo pyridyl ligand and a Ru-porphyrin. Alternatively, symmetrical bisporphyrins can be assembled through bridging either two Ga-porphyrins between a diacetylenic azo linker or two Ru-porphyrins between a bipyridyl azo linker.

Results and discussion

1. Synthesis. The assembly of the desired porphyrinic systems required ligands ***trans*-L1–L5** (Scheme 1). The synthesis of ***trans*-L3**,[16] ***trans*-L4**,[17] and ***trans*-L5**[18] has been reported, while the formation of ***trans*-L1** and ***trans*-L2**[19] are described in Scheme 1. The synthesis of ligand ***trans*-L1** began with the diazo-coupling reaction[20] of 4-acetamido-pyridine and 1-bromo-4-nitrobenzene to produce **1** in a moderate yield. Subsequent Sonogashira cross-coupling[21] of **1** with 2-methyl-3-butyn-2-ol gave **2**. The use of 2-methyl-3-butyn-2-ol as the alkyne source was required for the synthesis of ligand **2**, since incomplete conversion during the Sonogashira cross-coupling of **1** and trimethylsilylacetylene led to problematic separation and low yields. Liberation of the acetylene group was accomplished via reaction of **2** with NaOH in toluene (110 °C) and furnished the desired ligand ***trans*-L1**. Following an analogous strategy, the known azo compound **3**[22] was subjected to a Sonogashira cross-coupling reaction with trimethylsilylacetylene to give **4**, followed by deprotection with K_2CO_3 to give ligand ***trans*-L2** in excellent yield.

10.1002/chem.202002030

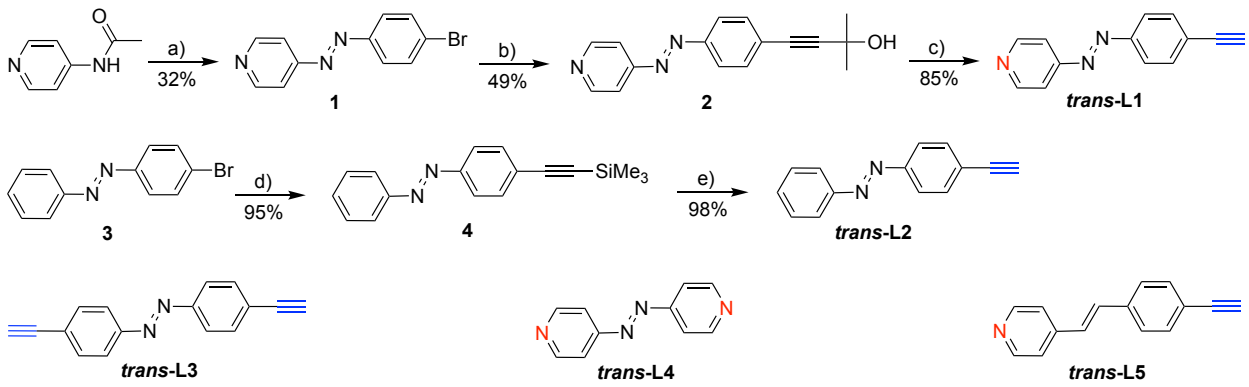

Scheme 1. Synthesis of azo ligands ***trans*-L1** and ***trans*-L2** and structures of ***trans*-L3**, ***trans*-L4**, and ***trans*-L5**. Reagents and conditions: a) NaOH, K_2CO_3, tris[2-(2-methoxyethoxy)ethyl]amine, 1-bromo-4-nitrobenzene, xylene, 130 °C; b) $PdCl_2(PPh_3)_2$, CuI, Et_2NH , 2-methyl-3-butyn-2-ol, 45 °C; c) NaOH, toluene, 110 °C; d) $PdCl_2(PPh_3)_2$, CuI, Et_3N, trimethylsilylacetylene, 45 °C; e) K_2CO_3, $MeOH/CH_2Cl_2$, rt.

Initial attempts to assemble **GaL1** used *n*BuLi to form the acetylide from ***trans*-L1** (5 equiv) followed by reaction with Ga(tpfpp)Cl (**5**).[23] This approach, however, was unsuccessful and led to a complex, unidentifiable mixture. Ligand ***trans*-L1** could be recovered from the resulting reaction mixture, but desired product could not be isolated chromatographically (silica gel, alumina, or size exclusion). On the other hand, using lithium bis(trimethylsilyl)amide (LiHMDS) smoothly gave the acetylide from ***trans*-L1**, which was then treated with porphyrin **5** in a solution of THF, and isolation of the product by size exclusion chromatography gave good yield of **GaL1** (Scheme 2). It is noted that the incorporation of perfluorophenyl groups in the *meso*-positions of the porphyrin increases persistence of the resulting complexes in comparison to nonfluorinated arenes, as a result of a stronger metal–acetylide bond.[10]

As a model compound for comparison to **GaL1** that does not contain the coordinating pyridyl ligand, complex **GaL2** was prepared in 93% yield via lithiation of ***trans*-L2** with *n*BuLi and addition to porphyrin **5** in a solution of toluene. Both compounds, **GaL1** and **GaL2** are stable solids that slowly hydrolyze in solution to liberate the free azo ligand, presumably due to the presence of adventitious water.

10.1002/chem.202002030

As observed in efforts to form **GaL1**, using *n*BuLi to form the acetylide of ***trans*-L3** and subsequent reaction with porphyrin **5** failed to give the target complex **GaL3Ga**. Formation of **GaL3Ga** was, however, successful using LiHMDS to form the acetylide although only very low yields could be isolated pure (4%). In attempts toward optimization, the deprotonation process was examined through formation of the acetylide with either *n*BuLi or LiHMDS and quenching with D_2O (see Figure S77 for details). The former reaction gave an unidentified mixture of products based on characterization by ^{1}H NMR spectroscopy, while the later reaction gave deuterated ***trans*-L3** suggesting that the acetylide had successfully been formed. Nevertheless, the reaction to form **GaL3Ga** could not be easily optimized, and additional efforts were abandoned.

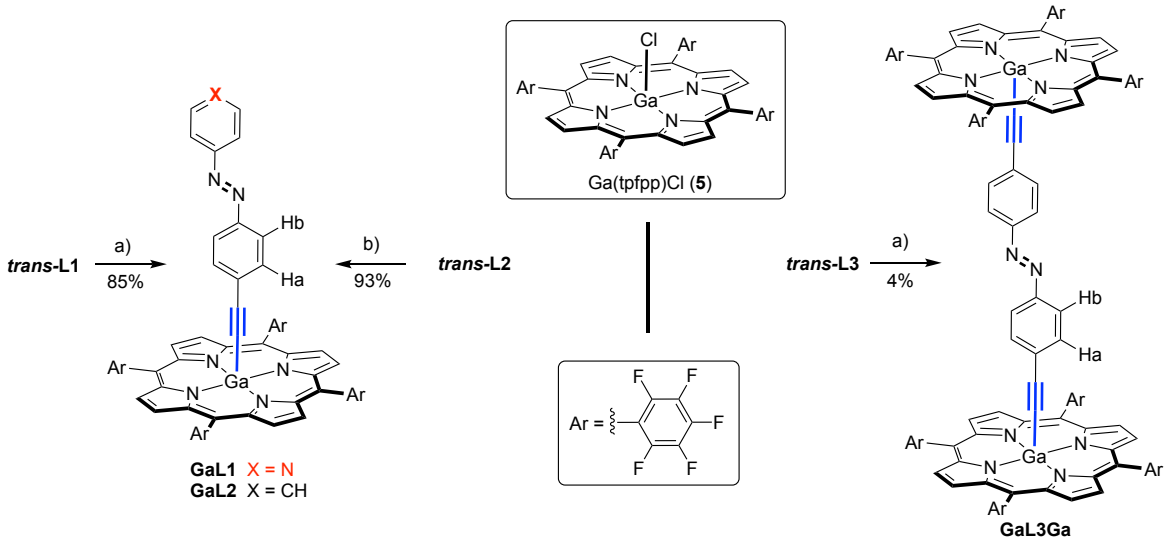

Scheme 2. Synthesis of porphyrins **GaL1**, **GaL2**, and **GaL3Ga**. Reagents and conditions: a) LiHMDS, then Ga(tpfpp)Cl (**5**), THF, –78 °C to rt; b) *n*BuLi in hexanes, then **5**, toluene/THF (5:2), –78 to 50 °C.

The pyridyl groups in derivatives ***trans*-L1** and ***trans*-L4** allow for an alternative approach toward a platform design, namely through coordinative self-assembly between the pyridyl group and a second metalloporphyrin. A Ru-metalloporphyrin with a CO ligand was chosen since pyridyl coordination to the metalloporphyrin is known to be strong and ligand-exchange slow,[24] which is advantageous when constructing porphyrin assemblies in solution (Scheme 3).[25] Thus, **RuL1** and **RuL4Ru** were formed by the complexation of Ru(tpfpp)(CO)(MeCN) (**6**) with ***trans*-L1** and

10.1002/chem.202002030

***trans*-L4**, respectively, and the products purified isolated in good yields by column chromatography. Finally, the strategic expansion of the framework of the **GaL1** was then targeted, and the bimetallic porphyrin system **GaL1Ru** was formed through reaction of platform **GaL1** with porphyrin **6** in toluene. The product could be isolated pure by size-exclusion chromatography, to give **GaL1Ru** in 44% yield as a dark red solid that was stable >1 year when stored either as a solid at rt or as a frozen solution in benzene under refrigeration (–20 °C). Finally, **GaL5Ru** was formed from ***trans*-L5** through an analogous stepwise protocol as a model compound to **GaL1Ru** that lacks the azo moiety.

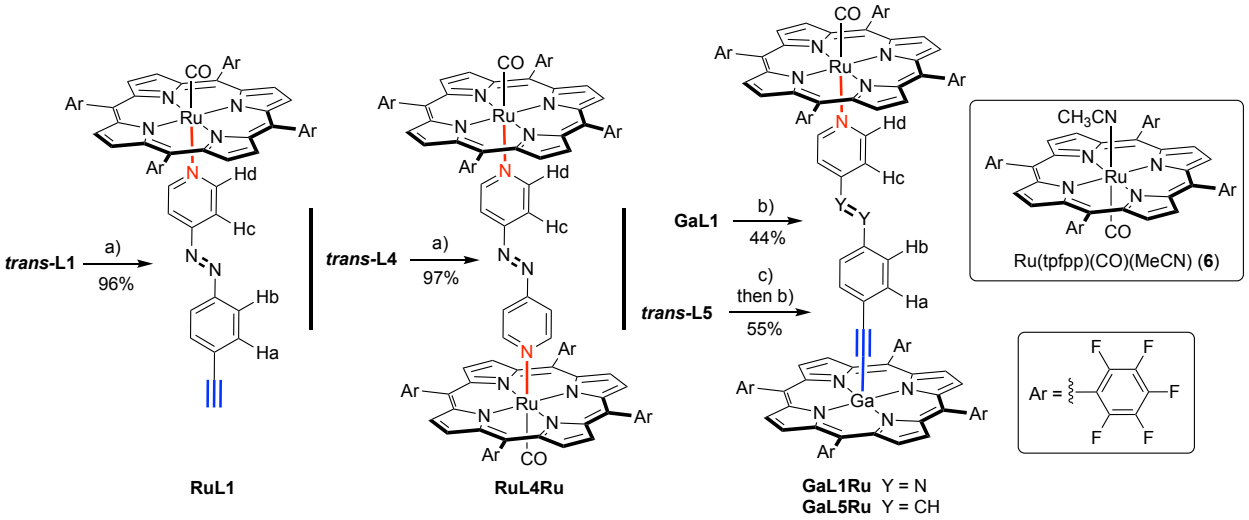

Scheme 3. Synthesis of porphyrins **RuL1**, **RuL4**, **GaL1Ru**, and **GaL5Ru**. Reagents and conditions: a) Ru(tpfpp)(CO)(MeCN) (**6**), CH_2Cl_2, rt; b) **6**, toluene, 50 °C; c) LiHMDS, then Ga(tpfpp)Cl (**5**), THF, –78 °C to rt.

The formation of **GaL1**, **GaL2**, **GaL3Ga**, **GaL1Ru**, **GaL5Ru**, **RuL1**, and **RuL4Ru** has been confirmed by mass spectrometry (MS) combined with ^{1}H, ^{13}C, ^{19}F, and 2D (^{1}H–^{1}H COSY, HSQC, HMBC) NMR spectroscopic analyses. A common feature of the spectroscopic characterization of all axial-bonded complexes is the dramatic "upfield" shift of the aryl protons of the ligands (Ha–Hd) in the ^{1}H NMR spectra as a result of diamagnetic shielding from the porphyrin (see Schemes 2 and 3 for proton labelling). Furthermore, individual resonances of all five fluorine atoms of the

meso-pentafluorophenyl groups are found in the ^{19}F NMR spectra with the expected F–F coupling. Inequivalence of the fluorine atoms of the *meso*-aryl groups is significant, as it confirms that dissociation of the axial ligands from the Ga- and Ru-porphyrin does not occur (at least on the timescale of the NMR experiments). Finally, strong signals are observed for $[M^+]$ at *m*/*z* 1247.0402, 1246.0439, 2310.0063 for **GaL1**, **GaL2**, and **GaL3Ga**, respectively, in the atmospheric pressure photoionization (APPI) HRMS analysis. Complexes **GaL1Ru**, **RuL1**, and **RuL4Ru**, on the other hand, typically show loss of the Ru-porphyrin moiety under APPI MS analysis, along with fragmentation patterns consistent with their proposed structure. It is noted that UV-vis and NMR spectroscopic characterization, supported by X-ray crystallography, conclusively corroborates the clean conversion of the *trans*-ligand to the *trans*-isomer of **GaL1**, **GaL2**, **GaL3Ga**, **GaL1Ru**, **RuL1**, and **RuL4Ru** (see SI for discussion).[26]

2. X-ray analyses. X-ray crystallographic analysis has been successful for **RuL1** and **RuL4Ru**, confirming both the proposed structure and stereochemistry about the azo moiety (Figure 1). In both molecules, the Ru-porphyrin features slightly distorted, six-coordinate octahedral geometry. The carbon and nitrogen framework of porphyrin ring is essentially planar in both cases, and the mean deviations from the least-squares planes (porphyrin-*N,N,N,N*-plane) fall within the range of –0.106(9) to 0.078(7) Å for **RuL1** and –0.220(5) to 0.039(4) Å for **RuL4Ru**. The Ru atom is situated above this plane by 0.061(2) Å and 0.0718(10) Å for **RuL1** and **RuL4Ru**, respectively. The axial pyridyl ligands are close to perpendicular to the porphyrin rings with N(py)–Ru–N(pyrrole) angles ranging from 87.61(16)° to 88.74(16)° for **RuL1** and 86.12(8)° to 89.31(8)° for **RuL4Ru**. Furthermore, the N(py)–Ru–C(CO) angles of **RuL1** and **RuL4Ru** are nearly linear at 177.6(2)° and 179.22(11)°, respectively. With respect to the ligand, the dihedral angle between the pyridyl and the phenylene ring of ***trans*-L1** is only 13.9(2)°, while the two pyridyl rings of ***trans*-L4** are coplanar (as determined by planes generated from the six atoms of the aryl groups of the linkers). Finally, the solid-state structures highlight that the presence of the CO ligand complicates

the use of Ru-porphyrins as part of a platform strategy, although the photochemical removal of the CO group is possible (*vide infra*).[13g, 27]

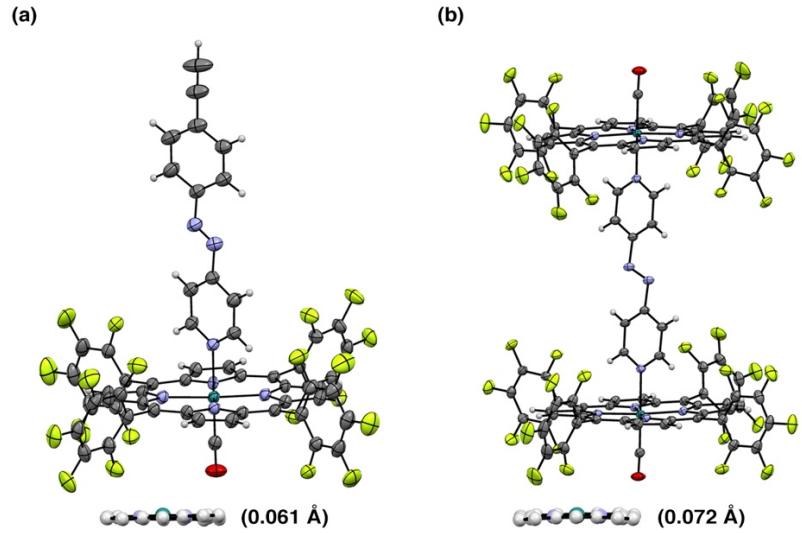

Figure 1. Top: ORTEP drawing of (a) **RuL1** and (b) **RuL4Ru**. Bottom: Side view of the porphyrin rings and the displacement (Å) of Ru atom out of the plane of the porphyrin for (a) **RuL1** and (b) **RuL4Ru**. Thermal ellipsoids drawn at 30% probability; gray carbon, red oxygen, lime green fluorine, purple nitrogen, white hydrogen, green ruthenium; CCDC 1999060 (**RuL1**) 1999059 (**RuL4Ru**).

3. ^{1}H NMR Characterization. The β-protons of the Ga-porphyrins of **GaL1** and **GaL2** are easily assigned as the most downfield singlets with an integration of 8H and an identical chemical shift at δ 8.94. The resonances of the β-protons are shifted slightly upfield to δ 8.86 in sandwich complexes of **GaL1Ru** and **GaL3Ga** upon addition of the second porphyrin. Likewise, the chemical shift of the β-protons for the Ru-porphyrins of **GaL1Ru** (δ 8.54) and **RuL4Ru** (δ 8.52) are shifted slightly upfield from those of **RuL1** (δ 8.65) by a similar amount (ca. 0.1 ppm). Thus, the β-protons appear to experience a slight effect from diamagnetic anisotropy (DA) over a distance of almost 1.3 nm from the second porphyrin, as estimated from the crystal structure of **RuL4Ru** (see Figure S3 for details).

The assignment of individual protons of the azo ligands used in the formation of the platforms is reasonably straightforward. A comparison of coupling patterns and constants allows separation into independent spin systems, Ha/Hb and Hc/Hd, while HMBC experiments reveal ^{3}J correlations between Ha and the neighboring acetylenic carbon that allows the distinction between Ha and Hb (see SI for details). In the case of ***trans*-L2**, COSY experiments show that the correlation of Hd ↔ Hp (Hp the proton at the *para* position of ***trans*-L2**) is stronger than that of Hc ↔ Hp, providing the identification of Hc and Hd, while analysis of HSQC and HMBC spectra of ***trans*-L1** allows distinction of Hc and Hd (see SI for details).

The protons Ha–d of ligands of metalloporphyrins are consistently shifted upfield in comparison to those of the free azo ligands, respectively, as expected due to the DA of the metalloporphyrins (Table 1). For example, protons Ha–d of free ligand ***trans*-L1** are found at δ 7.37, 7.68, 7.38, 8.63, respectively, and they are shifted to δ 7.05, 6.95, 5.01, and 1.74 in **RuL1**. A comparison of **GaL1** and **GaL2** to the free ligands ***trans*-L1** and ***trans*-L2** verifies that the influence of the Ga-porphyrin on each ligand is nearly the same. Protons Ha/Hb are shifted from δ 7.37/7.68 and 7.40/7.78 in ***trans*-L1** and ***trans*-L2**, respectively, to δ 5.40/5.43 and 6.72/6.82 for **GaL1** and **GaL2**, respectively.

The "sandwich" structure of **GaL1Ru**, **GaL3Ga**, and **RuL4Ru** provides a stronger shielding environment to the ligand when the second porphyrin is added. As an example, signals for Ha–d of **GaL1Ru** at δ 5.09, 6.00, 4.62, and 1.49 are shifted upfield when compared with **GaL1** (δ 5.40, 6.72, 6.99, and 8.38) and **RuL1** (δ 7.05, 6.95, 5.01, and 1.74), which show that the effects on proton resonances resulting from the Ga-porphyrin and Ru-porphyrin are approximately cumulative (see Table S1 for details). Two further examples also confirm this trend, namely the symmetrical bisporphyrinic systems **GaL3Ga** (Ha/Hb, δ 5.20/6.37) and **RuL4Ru** (Hc/Hd, δ 5.03/1.32) in comparison to **GaL1** (Ha/Hb, δ 5.40/6.72) and **RuL1** (Hc/Hd, δ 5.01/1.74); although the slightly different ligand structure affects somewhat the direct comparison.

10.1002/chem.202002030

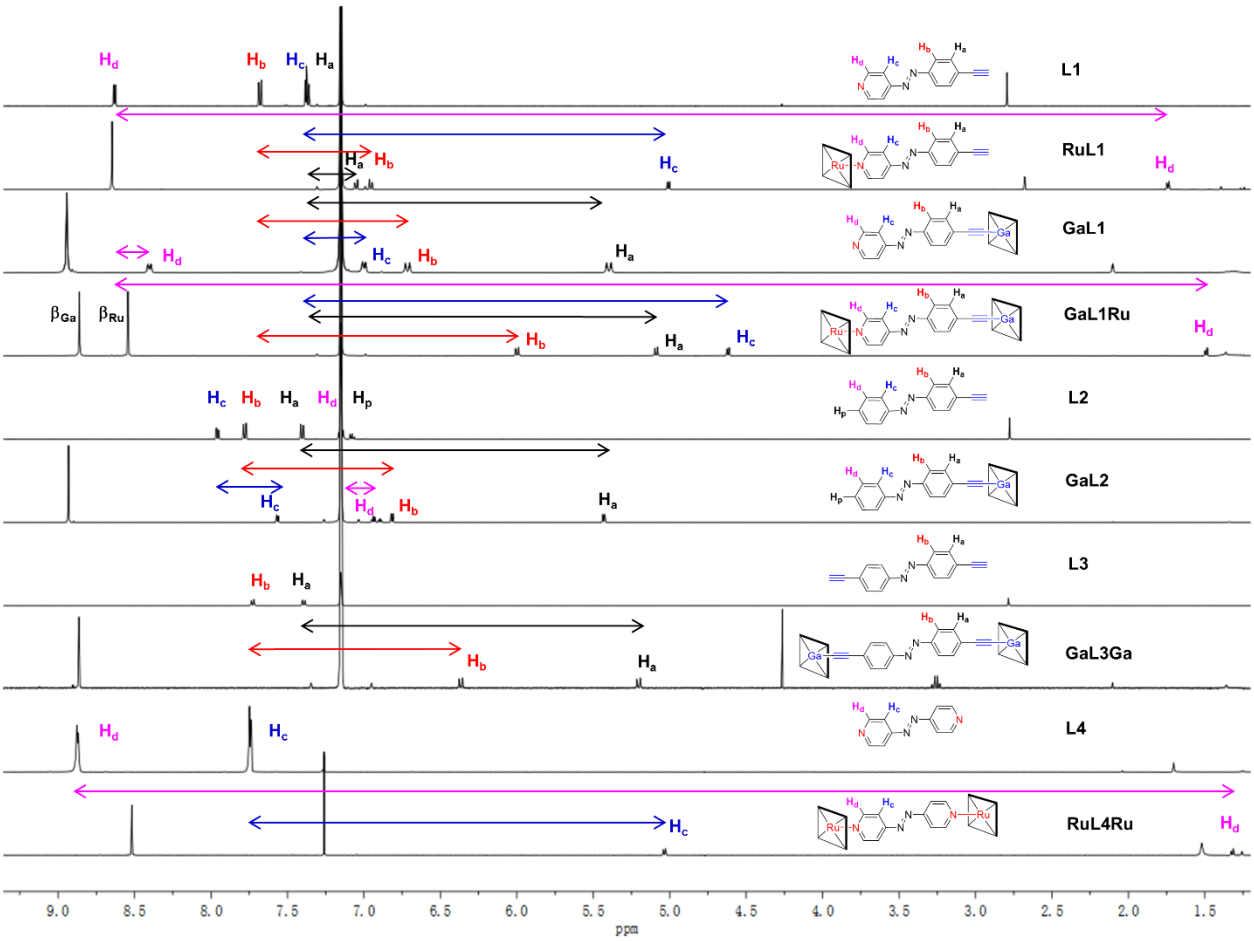

Figure 2. ^{1}H NMR spectra of ***trans*-L1**, **RuL1**, **GaL1**, **GaL1Ru**, ***trans*-L2, GaL2**, ***trans*-L3**, and **GaL3Ga** in C_6D_6 and ***trans*-L4** and **RuL4Ru** in $CDCl_3$. Arrows designate the change of chemical shift between free ligand and the resulting porphyrin complex.

Table 1. Selected ^{1}H NMR chemical shifts of ***trans*-L1**, **GaL1**, **RuL1**, **GaL1Ru**, ***trans*-L2**, **GaL2**, ***trans*-L3**, **GaL3Ga** in C_6D_6 and ***trans*-L4**, **RuL4Ru (**ppm, in $CDCl_3$).

proton	**L1**	**GaL1**	**RuL1**	**GaL1Ru**	**L2**	**GaL2**	**L3**	**GaL3Ga**	**L4**[a]	**RuL4Ru**[a]
Ha	7.37	5.40	7.05	5.09	7.40	5.43	7.39	5.20	—	—
Hb	7.68	6.72	6.95	6.00	7.78	6.82	7.73	6.37	—	—
Hc	7.38	6.99	5.01	4.62	7.96	7.57	—	—	7.74	5.03
Hd	8.63	8.38	1.74	1.49	7.15[b]	6.94	—	—	8.88	1.32
β-H	—	8.94	8.65	8.86/8.54	—	8.94	—	8.86	—	8.52

[a] measured in $CDCl_3$, [b] Signals are coincident with C_6D_6.

It is interesting to consider a simple, predictive analysis for the cumulative effects from DA on chemical shifts of ligand protons as a function of distance, *r*, of the proton from the porphyrins. This general topic has been discussed in the literature, and these studies suggest that such estimates can be complicated by both orientation of the proton in the "shielding cone" of the porphyrin coupled with the distance from the porphyrin.[28] More recently, Stanger has shown that, based on $NICS_{\pi,zz}$ calculations, at distance *r* greater than 2 Å, the maximum DA is found approximately at the geometrical center above the aromatic molecule.[29] Adapting the proposal of Stanger to analysis of experimental chemical shifts suggests that the effect of DA can be approximated through the relationship of $\Delta\delta(r)$, in which *r* is the distance of the proton from the plane of the aromatic system. The experimental data is thus fit to a two-parameter power law of the form:

$$\Delta\delta(r) = ka^r \qquad \text{eq (1)}$$

in which $\Delta\delta(r)$ represents change in chemical shift in the presence of DA from the porphyrin at distance *r*, '*a*' and '*k*' are fitting parameters, and '*k*' indicates how fast the anisotropy effect decays versus distance. Importantly, as $r \rightarrow \infty$, a limiting value of $\Delta\delta_\infty = 0$ is achieved, and the effects of DA are no longer discernible by the NMR measurement.[30]

The effects of DA arising from a Ru-porphyrin could be evaluated using **RuL1** and considering the difference in chemical shift between free ligand and the porphyrin complexes, $\Delta\delta$ (in ppm) as a function of the distance (*r* in Å) of protons to the porphyrin plane. Values of *r* are obtained by

calculating the distance between protons Ha–e and a plane generated from 24 carbon and nitrogen atoms of Ru-porphyrin in the solid-state structure.

Using $\Delta\delta$ and r values for **RuL1**, analysis of these values using eq (1) gives $a = 0.61 \pm 0.03$, $k = 22.75 \pm 2.64$ when the experimental data were measured in $CDCl_3$ (see Figure S2 for details). As a test, eq (1) was applied to the sandwiched **RuL4Ru** system. The calculated values for protons ($\Delta\delta'$) in **RuL4Ru** were obtained by summing the contributions to diamagnetic shielding from the two Ru-porphyrins ($\Delta\delta(r_1)$ and $\Delta\delta(r_2)$) based on eq (1) using X-ray data to estimate r (i.e., $\Delta\delta' = \Delta\delta(r_1) + \Delta\delta(r_2)$, see Figure S3 and Table S3 for details). The analysis using eq (1) for **RuL4Ru** predicts upfield shifts of $\Delta\delta' = 7.48$ and 2.73 ppm for protons Hd and Hc, respectively, which match well to the experimentally measured values of 7.56 and 2.71 ppm. The slight deviations between calculated and experimental chemical shifts likely arise from the estimation of r using X-ray crystallographic data, which offers only a static analysis for a clearly dynamic system (e.g., via bond bending) in solution. The fit to eq (1) provides a quantitative analysis and nicely verifies the additive effect of the two porphyrin rings, although constants a and k would be both expected to vary with substrate and ligand. Finally, taking into account of the accuracy of the NMR spectroscopy (± 0.001 ppm), the anisotropy effect would be predicted to disappear at distances greater than 20.0 Å.[30]

4. Photophysical properties

Switching in ligand *trans*-L1 and *trans*-L2. Azobenzene derivatives are designed to show photoswitching under UV-vis irradiation,[31] and the investigation here begins with ***trans*-L1** and ***trans*-L2**, in order to establish a reference point for analysis of optoelectronic properties.[32] Ligands ***trans*-L1** and ***trans*-L2** show similar energies for the π–π* (λ_{max} = 333 nm) and n–π* (λ_{max} = 450 nm) bands, while the molar absorptivity of the π–π* band and n–π* band of ***trans*-L1** are weaker than those of ***trans*-L2** (see Figure S6). Selective irradiation of ***trans*-L1** and ***trans*-L2** at 365 and 450 nm effects reversible switching between *trans*- and *cis*-isomer, respectively. The photostationary state (PSS) is rapidly reached (2–5 min) for ***trans*-L1** and ***trans*-L2** upon

irradiation at 365 nm, while the reverse reaction is slower (4–4.5 h) upon irradiation at 450 nm. Absorptions centered at 333 nm of ***trans*-L1** and ***trans*-L2** are decreased upon isomerization to the *cis*-isomers, while peaks centered at 262 and 450 nm, characteristic of the *cis*-isomer, are increased (see Figure S7). Irradiation of either ***trans*-L1** or ***trans*-L2** at 365 nm in an NMR tube produced predominantly ***cis*-L1** and ***cis*-L2** at the PSS (63 and 90% yield, respectively), while subsequent irradiation of the resulting *cis/trans*-isomeric mixture at 450 nm reversed the switching to return to primarily ***trans*-L1** and ***trans*-L2** at the PSS (92 and 85% yield, respectively, see Figures S27 and S35).

Appending ***trans*-L1–L4** as axial ligands to either Ga- or Ru-porphyrins has little effect on the ground-state electronic makeup of either the ligand or the metalloporphyrin, and absorption spectra of the *trans*-complexes are effectively a sum of their parts. Noticeable features from the spectra of **GaL1**, **RuL1**, **GaL1Ru**, **GaL2**, **GaL3Ga**, **RuL4Ru**, and **GaL5Ru** include Soret bands at 404–405 nm and at 422 nm for Ru- and Ga-porphyrins, respectively (Figure 3a). The UV-vis spectrum of mixed-metal bisporphyrin **GaL1Ru** shows two completely separate Soret bands centered at 405 nm (ε = 398000 $M^{-1}cm^{-1}$) and 422 nm (ε = 505000 $M^{-1}cm^{-1}$) assigned to the Ru- and Ga-porphyrins, respectively (Figure 3a). The two separate Soret bands are also observed for **GaL5Ru** in CH_2Cl_2, centered at 406 nm (ε = 426000 $M^{-1}cm^{-1}$) and 422 nm (ε = 478000 $M^{-1}cm^{-1}$). Split Soret bands have been reported by Osuka and coworkers for a series of *meso*-*meso*-linked bisporphyrins, derived from exciton coupling.[33] It is unlikely that exitonic coupling is operative in **GaL1Ru**, however, as the Ru-porphyrin and Ga-porphyrin have quite independent absorptions and little electronic communication in the ground state. More specifically, a linear combination of the spectra of **GaL1Ru** and **L1** is essentially equivalent to the summation of the spectra of **GaL1** and **RuL1** (see Figure S4).

Switching in platforms with either Ga- or Ru-porphyrins. Azo ligands appended to metalloporphyrins are expected to undergo photoisomerization (Figure 3b).[1b, 4b, 12a] Unfortunately, the photoisomerization of platforms ***trans*-GaL1** and ***trans*-GaL2** was essentially suppressed upon irradiation at 365 nm (see Figures S8–S9 for details). Ruthenium complexes with azo dyes have

been reported to be photoswitchable,[34] suggesting that systems based on axial bonding to a Ru-porphyrin might be more efficiently switched. Upon irradiation at 360 nm in toluene solution, ***trans*-RuL1** and ***trans*-RuL4Ru** exhibit obvious changes in their UV-vis spectra. Specifically, irradiation of ***trans*-RuL1** and ***trans*-RuL4Ru** results in a reduction of the Soret bands at the PSS (centered at 407 nm and 405 nm and reduced ca. 15% and 13%, respectively), and the concurrent emergence of a broad absorption between 560–800 nm (see Figures S10 and S11 for details). The PSS for **RuL1** is reached by 130 min and by 210 min for **RuL4Ru**, which is significantly longer than that for the unbound ligands ***trans*-L1** and ***trans*-L2** (*vide supra*). The new, broad absorption at low energy was tentatively assigned as a metal-to-axial ligand charge-transfer (MLCT) band, as has been suggested by Marvaud and Launay for Ru-porphyrins with axially bonded 4,4'-azopyridines.[13g] The thermal reversibility of the switching was then explored. After reaching the PSS, irradiation was discontinued, and the resulting solutions of **RuL1** and **RuL4Ru** were allowed to stand in the dark. This resulted in slight recovery of the initial UV-vis spectrum of both platforms ***trans*-RuL1** and ***trans*-RuL4Ru**, but the switching processes was mainly irreversible under thermal conditions (see Figures S10–S11 for details).

To probe the origin of the low energy bands from photoisomerization, a control experiment was designed with **RuL1**. A mixture of ***trans/cis*-L1** at the PSS was obtained by the irradiation of pure ***trans*-L1** (see SI). This isomeric mixture of **L1** was then titrated to a solution of porphyrin **6** in toluene. Indeed, a weak and broad peak was observed at 600–800 nm that increased in intensity as a function of the concentration of ***trans/cis*-L1**, suggesting the formation of a mixture of ***trans/cis*-RuL1** (see Figure S12a). As a comparison, ***trans*-L1** was also titrated to a solution of porphyrin **6** in toluene (see Figure S12b). The intensity of the low energy band in the control experiments was, however, weaker than that produced by direct irradiation of **RuL1** (see comparison in Figure S13). Therefore, emergence of the low energy, albeit weak, band during the photoirradiation of ***trans*-RuL1** is tentatively assigned to photoisomerization to ***cis*-RuL1** as well as photo-decarbonation (vide infra).

10.1002/chem.202002030

The inability to achieve reversible switching for **RuL1** and **RuL4Ru** suggested that competing photochemical processes were occurring. It was thus hypothesized that the switching experiments were complicated by photochemical decarbonylation, which is known for Ru-porphyrins and Ru-complexes.[13g, 27b, 27c, 35] and this possibility is discussed below.

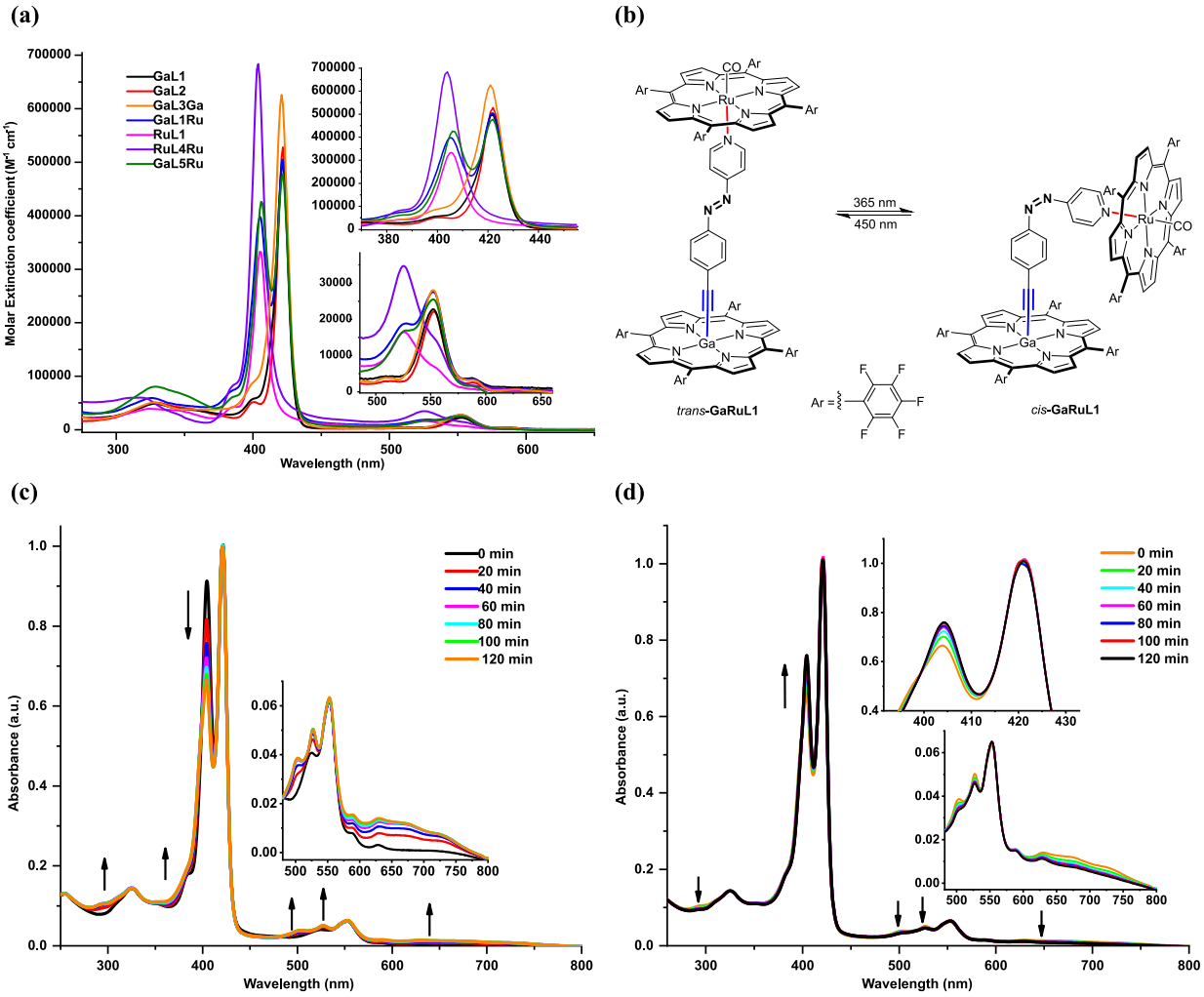

Figure 3. (a) Quantitative UV-vis spectra of **GaL1**, **GaL2**, **GaL3Ga**, **GaL1Ru**, **GaL5Ru**, **RuL1**, and **RuL4Ru** in CH_2Cl_2 solutions. (b) Schematic isomerization of complex **GaL1Ru**. UV-vis spectral changes of **GaL1Ru** upon irradiation at (c) 365 nm and then (d) 450 nm; hexanes solutions. See SI for experimental details.

Switching in platforms with both Ga- and Ru-porphyrins. In view of the lack of switching observed for **GaL1** combined with the weak switching for **RuL1** and **RuL4Ru** (*vide supra*), the photoisomerization of **GaL1Ru** inherently presented an interesting option since it featured a

combination of the two structural motifs. Irradiation of ***trans*-GaL1Ru** at 365 nm in a solution of hexanes results in a reduction (27%) and broadening in the Soret band arising from the Ru-porphyrin, while little change in the Soret band of the Ga-porphyrin is observed (Figure 3c). Concurrently, a new absorption centered at 500 nm appears, as well as a broad peak at 560–800 nm (as had been observed for **RuL1** and **RuL4Ru** and assigned as a MLCT band). The PSS was reached after irradiation for 2 h. Attempts to reverse the switching via irradiation at 450 nm (2 h) showed that, while the absorptions peaks trend toward the original spectrum of ***trans*-GaL1Ru**, the photoisomerization is clearly not completely reversible as shown in Figure 3d.[36]

The irradiation of the model compound **GaL5Ru** allows the decarbonylation process to be documented in the absence of azo switching. Specifically, irradiation of ***trans*-GaL5Ru** in a solution of hexanes results in a reduction in the Soret band of Ru-porphyrin (36%), while little change in the Soret band of the Ga-porphyrin is observed. A comparison of the behavior of **GaL1Ru** and **GaL5Ru** upon irradiation (Figure S16) highlights differences in the absence of the azo moiety and document both thermal and photochemical reversibility for **GaL1Ru** consistent with switching:

(a) Upon irradiation, intensity of the low energy absorptions of **GaL1Ru** (centered at ca. 502 and 525 nm) gradually increases as a function of time, while the absorption for **GaL5Ru** at ca. 525 nm gradually decreases.

(b) Upon irradiation, the Ru-Soret band of **GaL1Ru** shows decreased intensity that is accompanied by broadening of this absorption, while the intensity of Ru-Soret band of **GaL5Ru** decreases without broadening.

(c) After the PSS for **GaL1Ru** has been reached, changes in UV-vis spectra are observed by either allowing the sample to stand (without irradiation) or irradiation of the sample at 450 nm (Figure 3d and S17), and these changes are consistent with *cis-trans* isomerization. Changes to the spectra were not observed for **GaL5Ru** after allowing the sample to stand in the dark without irradiation.

Decarbonylation of Ru-porphyrins. The irreversible spectra changes for Ru-porphyrins after irradiation suggested the presence of a competing, chemical process during the switching experiments. The possibility of photochemical decarbonylation of the Ru-porphyrins[13g, 27b, 27c] was further explored using Ru(tpfpp)(CO)(pyridine) (**7**) as a simplified model in which pyridine replace with the azo-ligand.[37] Porphyrin **7** was irradiated at 360 nm in hexanes, and the photoinduced decarbonylation process was documented by monitoring the Soret band. The intensity was decreased by ca. 15% during the irradiation (ca. 1.5 h), concurrent with the appearance of a broad absorbance centered at ca. 700 nm. Under both thermal and photochemical conditions, the loss of CO was irreversible, and both the loss of intensity of the Soret band and the broad peak at lower energy (700 nm) persisted.

The decarbonylation process thus complicates analysis of photo-switching for systems that contain a Ru-porphyrin (**GaL1Ru, RuL1**, and **RuL4Ru**). In the case of **RuL1**, and **RuL4Ru**, decarbonylation appears to dominate, based on irreversible spectral changes after irradiation. Looking to the switching process for **GaL1Ru**, irradiation at 365 nm (hexanes) results in 27% reduction of the Soret band, while subsequent irradiation at 450 nm recovers to 44% of the original absorbance and the broad absorption at 600–800 nm discernibly diminishes. Thus, the photochemical switching of the azo group in **GaL1Ru** is a major contributor to the reversible process, while decarbonylation is a competing process. The system is, however, less than ideal.

Conclusions

In summary, the synthetic incorporation of azo groups into three bisporphyrin and three porphyrin assemblies via covalent bonding of axial ligands has been developed. All six systems are based on Ga- and/or Ru-metalloporphyrins toward developing switchable systems based on the "platform approach". The effects of diamagnetic anisotropy (DA) from the metalloporphyrins on the axial ligands has been examined, and the NMR chemical shifts of ligand protons can be effectively modelled using a power-law relationship based on the distance of the protons from the aromatic porphyrin core(s). The developed model shows that, in cases in which the ligand bridges two porphyrins, the effects of DA in the proton shift are additive.

Photophysical studies show that the photoisomerization of the azo moiety is ineffective for complexes bound to Ga-porphyrins (***trans*-GaL1** and ***trans*-GaL2**). Photoisomerization is also quite limited for those with only Ru-porphyrins as axial ligands (**RuL4R** and **RuL1**). Mixed metal, bisporphyrin **GaL1Ru** undergoes *trans*-/*cis*-isomerization upon irradiation, but similar to **RuL4R** and **RuL1**, the presence of the ruthenium carbonyl moiety complicates analysis of the photoisomerization due to irreversible photodecarbonylation. Thus, the formal addition of a Ga-porphyrin to **RuL1** to give **GaL1Ru** provides the most promising, switchable system, albeit the origin of this effect is not currently understood. Expansion of the versatile synthetic protocols developed herein will thus be directed to metalloporphyrins with enhanced photostability, in which the troublesome Ru-porphyrin is replaced by an alternative system such as, for example, a Zn-porphyrin or a B-subphthalocyanine.

Acknowledgements

We are grateful for funding from Natural Sciences and Engineering Research Council of Canada (NSERC), Canada Foundation for Innovation (CFI), and the Deutsche Forschungsgemeinschaft (SFB 953, "Synthetic Carbon Allotropes"). Y.G. acknowledges China Scholarship Council (CSC) funding. We thank Dr. Robert McDonald (X-ray structural determination), Dr. Mark Miskolzie (NMR spectroscopy), and Dr. Wayne Moffat (UV-vis spectroscopy) for the assistance with the measurements.

References

[1] a) M. Hammerich, R. Herges, *J. Org. Chem.* **2015**, *80*, 11233–11236; b) T. Muraoka, K. Kinbara, T. Aida, *Nature* **2006**, *440*, 512–515.

[2] a) A. S. Lubbe, W. Szymanski, B. L. Feringa, *Chem. Soc. Rev.* **2017**, *46*, 1052–1079; b) S. Samanta, A. A. Beharry, O. Sadovski, T. M. McCormick, A. Babalhavaeji, V. Tropepe, G. A. Woolley, *J. Am. Chem. Soc.* **2013**, *135*, 9777–9784; c) Q. Shao, B. Xing, *Chem. Soc. Rev.* **2010**, *39*, 2835–2846.

[3] a) A. Goulet-Hanssens, F. Eisenreich, S. Hecht, *Adv. Mater.* **2020**, e1905966; b) A. H. Heindl, J. Becker, H. A. Wegner, *Chem. Sci.* **2019**, *10*, 7418–7425.

[4] a) C. Zong, Y. Zhao, H. Ji, X. Han, J. Xie, J. Wang, Y. Cao, S. Jiang, C. Lu, *Angew. Chem. Int. Ed.* **2016**, *55*, 3931–3935; b) S. Venkataramani, U. Jana, M. Dommaschk, F. D. Sönnichsen, F. Tuczek, R. Herges, *Science* **2011**, *331*, 445–448; c) B. Baisch, D. Raffa, U. Jung, O. M. Magnussen, C. Nicolas, J. Lacour, J. Kubitschke, R. Herges, *J. Am. Chem. Soc.* **2009**, *131*, 442–443.

[5] A. Schlimm, R. Low, T. Rusch, F. Rohricht, T. Strunskus, T. Tellkamp, F. Sonnichsen, U. Manthe, O. Magnussen, F. Tuczek, R. Herges, *Angew. Chem. Int. Ed.* **2019**, *58*, 6574–6578.

[6] T. R. Rusch, M. Hammerich, R. Herges, O. M. Magnussen, *Chem. Commun.* **2019**, *55*, 9511–9514.

[7] S. Mohnani, D. Bonifazi, *Coord. Chem. Rev.* **2010**, *254*, 2342–2362.

[8] a) C. B. Kc, F. D'Souza, *Coord. Chem. Rev.* **2016**, *322*, 104–141; b) S. M. Law, D. Chen, S. L. Chan, X. Guan, W. M. Tsui, J. S. Huang, N. Zhu, C. M. Che, *Chem. Eur. J.* **2014**, *20*, 11035–11047.

[9] J. M. Kamm, C. P. Iverson, W. Y. Lau, M. D. Hopkins, *Langmuir* **2016**, *32*, 487–495.

[10] V. Walter, Y. Gao, N. Grzegorzek, M. Krempe, F. Hampel, N. Jux, R. R. Tykwinski, *Angew. Chem. Int. Ed.* **2019**, *58*, 494–498.

[11] a) C. Schutt, G. Heitmann, T. Wendler, B. Krahwinkel, R. Herges, *J. Org. Chem.* **2016**, *81*, 1206–1215; b) M. Dommaschk, C. Schutt, S. Venkataramani, U. Jana, C. Nather, F. D. Sonnichsen, R. Herges, *Dalton Trans.* **2014**, *43*, 17395–17405.

[12] a) W. Huang, S. K. Lee, Y. M. Sung, F. Peng, B. Yin, M. Ma, B. Chen, S. Liu, S. R. Kirk, D. Kim, J. Song, *Chem. Eur. J.* **2015**, *21*, 15328–15338; b) L. J. Esdaile, P. Jensen, J. C. McMurtrie, D. P. Arnold, *Angew. Chem. Int. Ed.* **2007**, *46*, 2090–2093; c) T. Yamamura, A. Momotake, T. Arai, *Tetrahedron Lett.* **2004**, *45*, 9219–9223; d) S. Tsuchiya, *J. Am. Chem. Soc.* **1999**, *121*, 48–53; e) H. K. Hombrecher, K. Lüdtke, *Tetrahedron* **1993**, *49*, 9489–9494.

[13] a) T. Hirose, F. Helmich, E. W. Meijer, *Angew. Chem. Int. Ed.* **2013**, *52*, 304–309; b) S. Dey, S. A. Ikbal, S. P. Rath, *New J. Chem.* **2014**, *38*, 1458–1470; c) J. Otsuki, E. Seki, T. Taguchi, M. Asakawa, K. Miyake, *Chem. Lett.* **2007**, *36*, 740–741; d) O. Tsutsumi, H. Sato, K. Takeda, T. Ogawa, *Thin Solid Films* **2006**, *499*, 219–223; e) J. Otsuki, K. Narutaki, *Bull. Chem. Soc. Jap.* **2004**, *77*, 1537–1544; f) J. Otsuki, K. Harada, K. Araki, *Chem. Lett.* **1999**, *28*, 269–270; g) V. Marvaud, J. P. Launay, *Inorg. Chem.* **1993**, *32*, 1376–1382.

[14] a) D. R. Reddy, B. G. Maiya, *J. Phys. Chem. A* **2003**, *107*, 6326–6333; b) D. R. Reddy, B. G. Maiya, *Chem. Commun.* **2001**, 117–118.

[15] S. Yao, Y. Yan, K. L. Wong, K. S. Chan, Z. Shen, *J. Porphyr. Phthalocyanines* **2018**, *22*, 918–924.

[16] L.-X. Liao, F. Stellacci, D. V. McGrath, *J. Am. Chem. Soc.* **2004**, *126*, 2181–2185.

[17] O. K. Farha, C. D. Malliakas, M. G. Kanatzidis, J. T. Hupp, *J. Am. Chem. Soc.* **2010**, *132*, 950–952.

[18] I.-Y. Wu, J. T. Lin, J. Luo, S.-S. Sun, C.-S. Li, K. J. Lin, C. Tsai, C.-C. Hsu, J.-L. Lin, *Organometallics* **1997**, *16*, 2038–2048.

[19] M. E. Moustafa, P. D. Boyle, R. J. Puddephatt, *Can. J. Chem.* **2014**, *92*, 706–715.

[20] N. R. Ayyangar, S. N. Naik, K. V. Srinivasan, *Tetrahedron Lett.* **1989**, *30*, 7253–7256.

[21] R. R. Tykwinski, *Angew. Chem. Int. Ed.* **2003**, *42*, 1566–1568.

[22] O. Zenkina, M. Altman, G. Leitus, L. J. W. Shimon, R. Cohen, M. E. van der Boom, *Organometallics* **2007**, *26*, 4528–4534.

[23] J. S. Lindsey, R. W. Wagner, *J. Org. Chem.* **1989**, *54*, 828–836.

[24] K. Chichak, N. R. Branda, *Chem. Commun.* **1999**, 523-524.

[25] a) M. Krempe, R. Lippert, F. Hampel, I. Ivanovic-Burmazovic, N. Jux, R. R. Tykwinski, *Angew. Chem. Int. Ed.* **2016**, *55*, 14802–14806; b) K. Campbell, R. McDonald, N. R. Branda, R. R. Tykwinski, *Org. Lett.* **2001**, *3*, 1045–1048.

[26] Complexes **GaL1**, **GaL2**, **GaL3Ga**, **GaL1Ru**, **RuL1**, and **RuL4Ru** refer to the *trans*–isomer unless specifically labelled as the *cis*–isomer.

[27] a) N. Shafizadeh, S. Boye-Peronne, S. Soorkia, B. K. Cunha de Miranda, G. A. Garcia, L. Nahon, S. Chen, A. de la Lande, L. Poisson, B. Soep, *Phys. Chem. Chem. Phys.* **2018**, *20*, 11730–11739; b) K. Ishii, S.-i. Hoshino, N. Kobayashi, *Inorg. Chem.* **2004**, *43*, 7969–7971; c) M. Hoshino, Y. Kashiwagi, *J. Phys. Chem.* **1990**, *94*, 673–678.

[28] a) H. Iwamoto, K. Hori, Y. Fukazawa, *Tetrahedron* **2006**, *62*, 2789–2798; b) Y. Uemori, A. Nakatsubo, H. Imai, S. Nakagawa, E. Kyuno, *Inorg. Chem.* **1992**, *31*, 5164–5171; c) R. J. Abraham, S. C. M. Fell, K. M. Smith, *Org. Magn. Reson.* **1977**, *9*, 367–373.

[29] A. Stanger, *J. Phys. Chem. A* **2019**, *123*, 3922–3927.

[30] A reasonable definition is required to establish when $\Delta\delta_\infty$ has been achieved. Assuming that the accuracy of the NMR measurements is ± 0.001 ppm, $\Delta\delta_\infty$ is defined by fulfilment of the relationship $\Delta\delta r - \Delta\delta r' \leqslant$ 0.001 ppm, i.e., $\Delta\delta_\infty$ has been achieved if the difference in chemical shifts at two distances, r and r' cannot be resolved by the NMR measurement.

[31] S. Crespi, N. A. Simeth, B. Koinig, *Nat. Rev. Chem.* **2019**, *3*, 133–146.

[32] a) R. A. Al-Balushi, A. Haque, M. Jayapal, M. K. Al-Suti, J. Husband, M. S. Khan, J. M. Skelton, K. C. Molloy, P. R. Raithby, *Inorg. Chem.* **2016**, *55*, 10955–10967; b) N. Masaru, R. Masahiro, W. Masayoshi, S. Kohei, O. Naoya, *Bull. Chem. Soc. Jap.* **1997**, *70*, 737–744.

[33] a) N. Fukui, H. Yorimitsu, A. Osuka, *Chem.* **2016**, *22*, 18476–18483; b) N. Yoshida, T. Ishizuka, A. Osuka, D. H. Jeong, H. S. Cho, D. Kim, Y. Matsuzaki, A. Nogami, K. Tanaka, *Chem. Eur. J.* **2003**, *9*, 58–75.

[34] K. Ghebreyessus, S. M. Cooper, *Organometallics* **2017**, *36*, 3360–3370.

[35] S. J. Carrington, I. Chakraborty, J. R. Alvarado, P. K. Mascharak, *Inorg. Chim. Acta* **2013**, *407*, 121–125.

[36] Thermal reversion was also minimal upon standing at room temperature, although the experiment was not quantified.

[37] Photophysical studies of multiporphyrin arrays incorporating Ru-metalloporphyrins bearing a CO ligand suggested that these systems would be stable under mild irradiation (see ref. 24), while decarbonylation is well known under strong irradiation (refs. 13g, 27b, 27c). In the present case, no attempt was made to identify the product(s) of decarbonylation given the small amounts that were produced in the experiments.

10.1002/chem.202002030

Entry for the Table of Contents

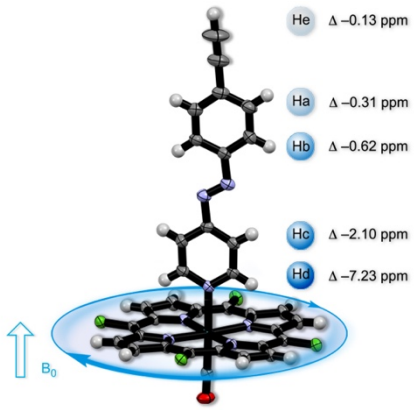

Porphyrin platforms. The hierarchical synthesis of mono- and bisporphyrinic systems is developed based on bonding of σ-acetylide ligands to Ga-porphyrins and coordination of pyridyl ligands to Ru-porphyrins. The effects of diamagnetic anisotropy on ^{1}H NMR shifts is modelled vs a combination of distance from the plane of the porphyrin and cumulative effects of two porphyrins. Incorporation of ligands featuring azo moieties offers switchable systems.

@TykwinskiGroup